

Organic sulfur fingerprint indicates continued injection fluid signature 10 months after hydraulic fracturing

Luek, J.L.^{1,2}, Harir, M.³, Schmitt-Kopplin, P.^{3,4}, Mouser, P.J.¹, Gonsior, M.²

¹ University of New Hampshire, Department of Civil and Environmental Engineering, USA

² University of Maryland Center for Environmental Science, Chesapeake Biological Laboratory, USA.

³ Helmholtz Zentrum Muenchen, Research Unit Analytical BioGeoChemistry, Neuherberg, Germany

⁴ Technische Universität München, Chair of Analytical Food Chemistry, Freising-Weihenstephan, Germany

*Corresponding author contact:

Jenna L. Luek, University of New Hampshire, Durham, NH 03825

+14126054898, Email address: jenna.luek@unh.edu

This supplemental file contains 7 tables, 11 figures, supplemental methods and results, and references.

Page 2 – Tables

Page 14 – Figures

Page 23 – Supplemental methods and results

Page 27 – References

Table S1. Descriptive statistical parameters for carbon oxidation state (CO_x) and molecular weight averages (MW_a) and weighted averages.

Days After Flowback Began	Number of CHOS ions	MW _a	Standard Deviation	Standard Error	MW _{wa}	Standard Deviation	Standard Error
Well 3H							
Frac Fluid	345	334	63	4	341	60	3.2
Frac Fluid	294	337	67	4	337	61	3.6
4	780	356	91	3	325	67	2.4
5	939	373	104	3	332	65	2.1
6	751	358	91	3	325	66	2.4
7	773	356	89	3	330	63	2.3
10	725	352	81	3	329	61	2.3
36	665	346	81	3	314	61	2.4
56	655	347	74	3	323	58	2.3
70	562	336	72	3	306	60	2.5
84	592	361	80	3	330	59	2.4
119	511	344	74	3	328	58	2.6
182	460	329	70	3	310	62	2.9
217	482	336	78	4	315	69	3.1
280	547	335	79	3	311	66	2.8
Well 5H							
Frac Fluid	90	328	78	8	327	79	8.3
Frac Fluid	132	332	62	5	331	64	5.6
10	663	357	81	3	332	56	2.2
14	811	365	92	3	324	61	2.1
36	963	377	107	3	320	64	2.1
56	809	380	105	4	333	61	2.1
70	756	370	104	4	312	62	2.2
119	526	335	69	3	312	62	2.7
280	596	343	79	3	307	68	2.8
Days After Flowback Began	Number of CHOS ions	CO _{x,a}	Standard Deviation	Standard Error	CO _{x,wa}	Standard Deviation	Standard Error
Well 3H							
Frac Fluid	345	-0.17	0.54	0.03	-0.23	0.49	0.06
Frac Fluid	294	-0.17	0.53	0.03	-0.21	0.50	0.06
4	780	-0.16	0.53	0.02	-0.26	0.41	0.04
5	939	-0.20	0.55	0.02	-0.75	0.47	0.05
6	751	-0.15	0.53	0.02	-0.40	0.49	0.05

7	773	-0.12	0.53	0.02	-0.34	0.47	0.05
10	725	-0.14	0.54	0.02	-0.35	0.48	0.05
36	665	-0.18	0.56	0.02	-0.28	0.45	0.05
56	655	-0.24	0.59	0.02	-0.39	0.50	0.06
70	562	-0.18	0.57	0.02	-0.40	0.52	0.06
84	592	-0.18	0.50	0.02	-0.33	0.44	0.05
119	511	-0.20	0.51	0.02	-0.41	0.47	0.05
182	460	-0.27	0.53	0.02	-0.35	0.48	0.06
217	482	-0.23	0.54	0.02	-0.29	0.47	0.05
280	547	-0.22	0.55	0.02	-0.41	0.53	0.06
Well 5H							
Frac Fluid	90	-0.34	0.55	0.06	-0.37	0.58	0.06
Frac Fluid	132	-0.17	0.44	0.04	-0.17	0.42	0.04
10	663	-0.17	0.50	0.02	-0.50	0.45	0.02
14	811	-0.16	0.52	0.02	-0.47	0.45	0.02
36	963	-0.21	0.53	0.02	-0.47	0.46	0.01
56	809	-0.30	0.56	0.02	-0.77	0.47	0.02
70	756	-0.15	0.53	0.02	-0.34	0.41	0.01
119	526	-0.19	0.55	0.02	-0.24	0.44	0.02
280	596	-0.24	0.51	0.02	-0.41	0.46	0.02

Table S2. Linear regression parameters for carbon oxidation state (COx) and molecular weight averages and weighted averages as a function of days after flowback began. *Note: Bolded values indicate significant regressions ($p < 0.05$).*

	5H COx_a	Std. Error	5H COx_{wa}	Std. Error	5H MW_a	Std. Error	5H MW_{wa}	Std. Error
Slope	-3.10E-05	2.90E-04	6.70E-05	7.30E-04	-0.03	0.085	-0.084	0.026
Intercept	-0.21	0.03	-0.42	0.078	356	9	327	2.8
R²	0		0		0.01		0.59	
Significance of Slope (p-value)	0.92		0.93		0.73		0.015	

	3H COx_a	Std. Error	3H COx_{wa}	Std. Error	3H MW_a	Std. Error	3H MW_{wa}	Std. Error
Slope	0.00031	8.7E-05	3.6E-05	0.00039	-0.1	0.0	-0.074	0.025
Intercept	-0.16	0.0097	-0.36	0.044	352	3.7	329	2.8
R²	0.50		0		0.275		0.41	
Significance of Slope (p-value)	0.003		0.93		0.045		0.01	

Table S3. Investigation of carbon and sulfur isotopes in abundant organic sulfur compound.

Formula	Exact Mass	Measured Mass	Mass Error (ppm)	Expected Intensity	Actual Intensity
$C_{16}H_{33}O_7S^-$	369.19525	369.19525	0	NA	4.62×10^9
$^{13}C_{16}H_{33}O_7S^-$	370.19859	370.19861	0.054	7.99×10^8	7.99×10^8
$C_{16}H_{33}O_7^{34}S^-$	371.19105	371.19107	0.054	2.03×10^8	2.11×10^8
$^{13}C_{16}H_{33}O_7^{34}S^-$	372.19442	372.19440	0.054	3.70×10^7	3.76×10^7

Table S4. Average ethoxylate chain length distribution for alcohol ethoxysulfate (AES) calculated as the weighted average of ion abundances (raw abundances shown in **Figures S1-S6**). Complete distribution for days 10 and 280 are shown in **Figure 4**.

Days After Flowback Began	3H AE_xS Weighted Average	Days After Flowback Began	5H AE_xS Weighted Average
4	2.90	<i>10</i>	<i>3.33</i>
5	2.70	13	3.10
6	2.66	36	2.98
7	2.71	56	2.73
<i>10</i>	<i>2.68</i>	<i>70</i>	<i>3.08</i>
36	2.64	119	2.80
56	2.55	<i>280</i>	<i>2.89</i>
70	2.34		
84	2.75		
119	2.75		
182	2.61		
217	2.66		
<i>280</i>	<i>2.56</i>		

Table S5. Metagenomes and bacterial genomes queried from the Joint Genome Institute database with the IMG/M system. Sequencing for all samples performed by JGI.

Domain	Sequencing Status	Study Name	Genome Name / Sample Name	IMG Genome ID	Genome Size * assembled	Gene Count *assembled
Metagenome	Draft	Subsurface microbial communities from deep shales in Ohio and West Virginia, USA	Subsurface microbial communities from deep shales in West Virginia, USA - MSEEL Well Study Marcellus 5H 2016_02_17	3300013018	73301315	119134
Metagenome	Draft	Subsurface microbial communities from deep shales in Ohio and West Virginia, USA	Subsurface microbial communities from deep shales in West Virginia, USA - MSEEL Well Study Marcellus 5H 2016_03_03	3300013016	24217903	43203
Metagenome	Draft	Subsurface microbial communities from deep shales in Ohio and West Virginia, USA	Subsurface microbial communities from deep shales in West Virginia, USA - MSEEL Well Study Marcellus 5H 2016_04_06	3300013021	64472640	139816
Metagenome	Draft	Subsurface microbial communities from deep shales in Ohio and West Virginia, USA	Subsurface microbial communities from deep shales in West Virginia, USA - MSEEL Well Study Marcellus 5H 2016_09_14	3300013017	35743880	68444
Metagenome	Draft	Subsurface microbial communities from deep shales in Ohio and West Virginia, USA	Subsurface microbial communities from deep shales in West Virginia, USA - MSEEL Well Study Marcellus	3300013020	74175323	130093

			3H_2016_04_06			
Metagenome	Draft	Subsurface microbial communities from deep shales in Ohio and West Virginia, USA	Subsurface microbial communities from deep shales in West Virginia, USA - MSEEL Well Study Marcellus 5H_2016_07_13	3300013019	39060901	127432
Metagenome	Draft	Subsurface microbial communities from deep shales in Ohio and West Virginia, USA	Subsurface microbial communities from deep shales in West Virginia, USA - MSEEL Well Study Marcellus 3H_2016_09_14	3300013015	16240183	30724
Bacteria	Draft	Subsurface microbial communities from deep shales in Ohio and West Virginia, USA	Halanaerobium congolense MSL44.2	2754412643	2628135	2557
Bacteria	Draft	Subsurface microbial communities from deep shales in Ohio and West Virginia, USA	Halanaerobium congolense MSL28	2754412645	2709071	2647
Bacteria	Draft	Subsurface microbial communities from deep shales in Ohio and West Virginia, USA	Halanaerobium saccharolyticum MSL 17.2	2740892607	3311460	3122
Bacteria	Draft	Subsurface microbial communities from deep shales in Ohio and West Virginia, USA	Halanaerobium saccharolyticum MSL 19.2	2740892608	3392875	3223

Bacteria	Draft	Subsurface microbial communities from deep shales in Ohio and West Virginia, USA	Halanaerobium saccharolyticum MSL 7	2765235836	3118345	2951
Bacteria	Draft	Subsurface microbial communities from deep shales in Ohio and West Virginia, USA	Halanaerobium saccharolyticum MSL 9.2	2754412424	3393776	3221
Bacteria	Draft	Deep subsurface shale carbon reservoir microbial communities from Ohio and West Virginia, USA	Halanaerobium congolense WG10	2642422546	2925280	2882
Bacteria	Draft	Deep subsurface shale carbon reservoir microbial communities from Ohio and West Virginia, USA	Halanaerobium congolense UTICA-S4D12	2700989664	2768198	2710
Bacteria	Draft	Deep subsurface shale carbon reservoir microbial communities from Ohio and West Virginia, USA	Halanaerobium saccharolyticum WC1	2770939461	3248193	3059

Table S6. Specific genes queried in Marcellus shale produced water metagenome given in **Table S4** and their raw abundances in each metagenome. Bolded term represents the term used in the JGI IMG/M database search.

Function name	KEGG Number	E.C. Number	Gene	Total Identified in Metagenome	Marcellus_5H_2016_02_17	Marcellus_5H_2016_03_03	Marcellus_3H_2016_04_06	Marcellus_5H_2016_04_06	Marcellus_5H_2016_07_13	Marcellus_3H_2016_09_14	Marcellus_5H_2016_09_14
<i>Days After Flowback Began</i>					70	84	119	119	217	280	280
Alkyl sulfatase				12	5	0	7	0	0	0	0
Alkyl sulfatase		3.1.6.19		0	0	0	0	0	0	0	0
Arylsulfatase			asIA	190	29	28	70	24	10	11	18
Arylsulfatase	K01130		asIA	18	4	0	10	3	0	0	1
Arylsulfatase		3.1.6.1	asIA	18	4	0	10	3	0	0	1
Sulfate transport system substrate-binding protein	K02048		CysP	34	18	3	6	4	1	1	1
Sulfate transport system permease protein	K02046		CysU	21	9	3	3	4	1	0	1
Sulfate transport system permease protein	K02047		CysW	20	10	1	2	4	2	0	1
sulfate transport system ATP-binding protein	K02045		CysA	23	10	3	4	3	1	1	1
Taurine transport system substrate binding protein	K15551		TauA	27	3	1	7	6	4	2	4
Taurine transport system permease protein	K15552		TauC	32	4	1	7	7	2	3	8
Taurine transport system ATP-binding protein	K10831		TauB	34	5	1	9	6	2	3	8

Alkanesulfonate transport system-substrate binding protein	K15553		ssuA	22	16	0	3	3	0	0	1
Alkanesulfonate sulfonate transport system permease protein	K15554		ssuC	24	7	2	4	3	2	3	3
Alkanesulfonate sulfonate transport system ATP-binding protein	K15555		ssuB	13	7	0	1	2	0	2	1
Cystine transport system substrate-binding protein	K02424		FliY	4	3	0	0	1	0	0	0
Cystine transport system permease protein	K10009		YecS	3	1	0	0	2	0	0	0
Cystine transport system ATP-binding protein	K10010		YecC	8	2	1	1	2	1	0	1
D-methionine transport system substrate-binding protein	K02073		MetQ	93	22	5	13	19	9	8	17
D-methionine transport system permease protein	K02072		MetI	53	17	4	9	9	4	4	6
D-methionine transport system ATP-binding protein	K02071		MetN	81	20	5	14	11	6	6	19
Alkanesulfonate monooxygenase	K04091		ssuD/msuD	21	13	0	8	0	0	0	0
Alkanesulfonate monooxygenase		1.14.14.5	ssuD/msuD	21	0	0	0	0	0	0	0
Taurine dioxygenase	K03119		tauD	20	4	0	14	0	0	2	0
Taurine dioxygenase		1.14.11.17	tauD	44	11	2	18	3	2	5	3
Taurine-pyruvate aminotransferase		2.6.1.77	tpa	0	0	0	0	0	0	0	0
Taurine dehydrogenase		1.4.99.2		0	0	0	0	0	0	0	0
Taurine: alpha-ketoglutarate aminotransferase		2.6.1.55		0	0	0	0	0	0	0	0
Sulfoacetaldehyde acetyltransferase		2.3.3.15	xsc	0	0	0	0	0	0	0	0

Table S7. Specific genes queried in Marcellus shale produced water and Utica shale produced water given in **Table S4** and their raw abundances in each metagenome. Bolded term represents the term used in the JGI IMG/M database search.

Function name	KEGG Number	E.C. Number	Gene	<i>Halanaerobium congolense</i> MSL 44.2	<i>Halanaerobium congolense</i> MSL 28	<i>Halanaerobium congolense</i> WG10	<i>Halanaerobium congolense</i> UTICA-S4D12	<i>Halanaerobium saccharolyticum</i> MSL 17.2	<i>Halanaerobium saccharolyticum</i> MSL 19.2	<i>Halanaerobium saccharolyticum</i> MSL 7	<i>Halanaerobium saccharolyticum</i> MSL9.2	<i>Halanaerobium saccharolyticum</i> WC1
Days After Flowback Began												
Alkyl sulfatase				0	0	0	0	0	0	0	0	0
Alkyl sulfatase		3.1.6.19		0	0	0	0	0	0	0	0	0
Arylsulfatase			asIA	X	0	0	0	X	X	0	X	0
Arylsulfatase	K01130		asIA	0	0	0	0	0	0	0	0	0
Arylsulfatase		3.1.6.1	asIA	0	0	0	0	0	0	0	0	0
sulfate transport system substrate-binding protein	K02048		CysP	0	0	0	0	0	0	0	0	0
Sulfate transport system permease protein	K02046		CysU	0	0	0	0	0	0	0	0	0
Sulfate transport system permease protein	K02047		CysW	0	0	0	0	0	0	0	0	0
sulfate transport system ATP-binding protein	K02045		CysA	0	0	0	0	0	0	0	0	0
Taurine transport system substrate binding protein	K15551		TauA	X	X	X	X	X	X	X	X	X
Taurine transport system permease protein	K15552		TauC	X	X	X	X	X	X	X	X	X

Taurine transport system ATP-binding protein	K10831		TauB	X	X	X	X	X	X	X	X	X
Alkanesulfonate transport system-substrate binding protein	K15553		ssuA	0	0	0	0	0	0	0	0	0
Alkanesulfonate sulfonate transport system permease protein	K15554		ssuC	0	0	0	0	0	0	0	0	0
Alkanesulfonate sulfonate transport system ATP-binding protein	K15555		ssuB	0	0	0	0	0	0	0	0	X
Cystine transport system substrate-binding protein	K02424		FliY	0	0	0	0	0	0	0	0	0
Cystine transport system permease protein	K10009		YecS	0	0	0	0	0	0	0	0	0
Cystine transport system ATP-binding protein	K10010		YecC	0	0	0	X	0	0	0	0	0
D-methionine transport system substrate-binding protein	K02073		MetQ	X	X	X	X	X	X	X	X	X
D-methionine transport system permease protein	K02072		MetI	X	X	X	X	X	X	X	X	X
D-methionine transport system ATP-binding protein	K02071		MetN	X	X	X	X	X	X	X	X	X
Alkanesulfonate monooxygenase	K04091		ssuD/msuD	0	0	0	0	0	0	0	0	0
Alkanesulfonate monooxygenase		1.14.14.5	ssuD/msuD	0	0	0	0	0	0	0	0	0
Taurine dioxygenase	K03119		tauD	0	0	0	0	0	0	0	0	0
Taurine dioxygenase		1.14.11.17	tauD	0	0	0	0	0	0	0	0	0
Taurine-pyruvate aminotransferase		2.6.1.77	tpa	0	0	0	0	0	0	0	0	0
Taurine dehydrogenase		1.4.99.2		0	0	0	0	0	0	0	0	0
Taurine:alpha-ketoglutarate aminotransferase		2.6.1.55		0	0	0	0	0	0	0	0	0
Sulfoacetaldehyde acetyltransferase		2.3.3.15	xsc	0	0	0	0	0	0	0	0	0

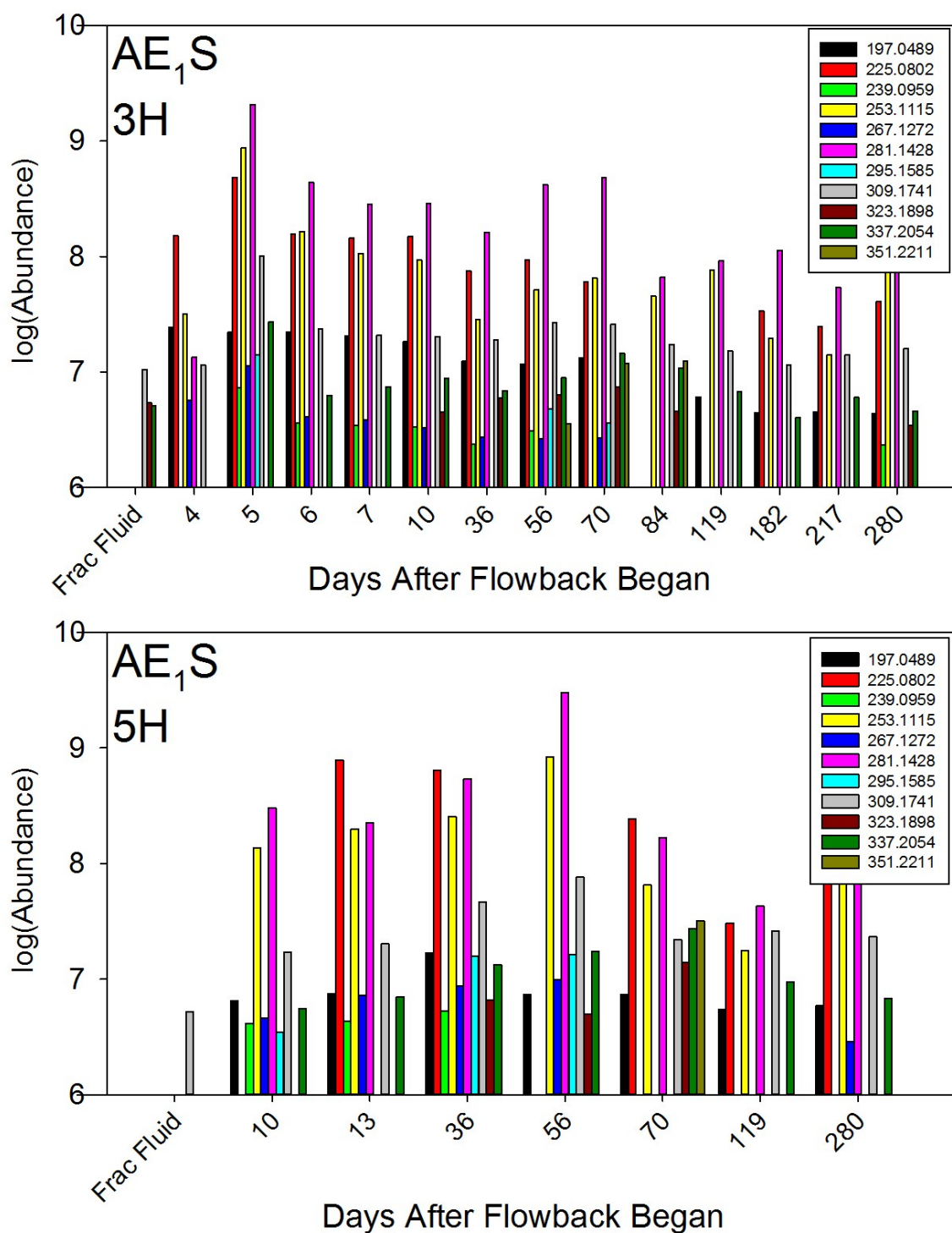


Figure S1. Distribution of ions corresponding to alcohol ethoxysulfate (AE_1S) homologous series in the MSEEL 3H (top) and 5H (bottom) well by days after flowback began.

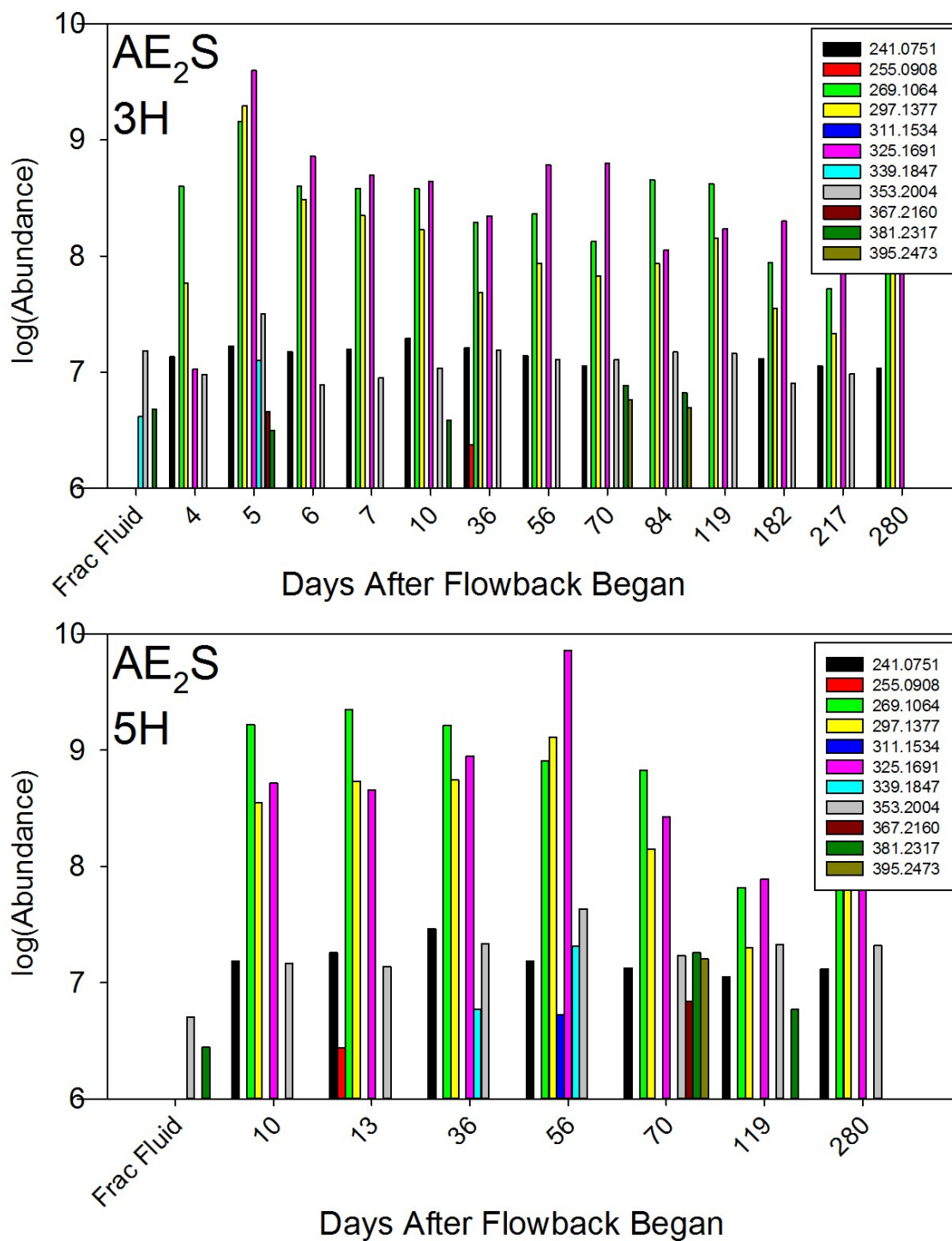


Figure S2. Distribution of ions corresponding to alcohol ethoxysulfate (AE_2S) homologous series in the MSEEL 3H (top) and 5H (bottom) well by days after flowback began.

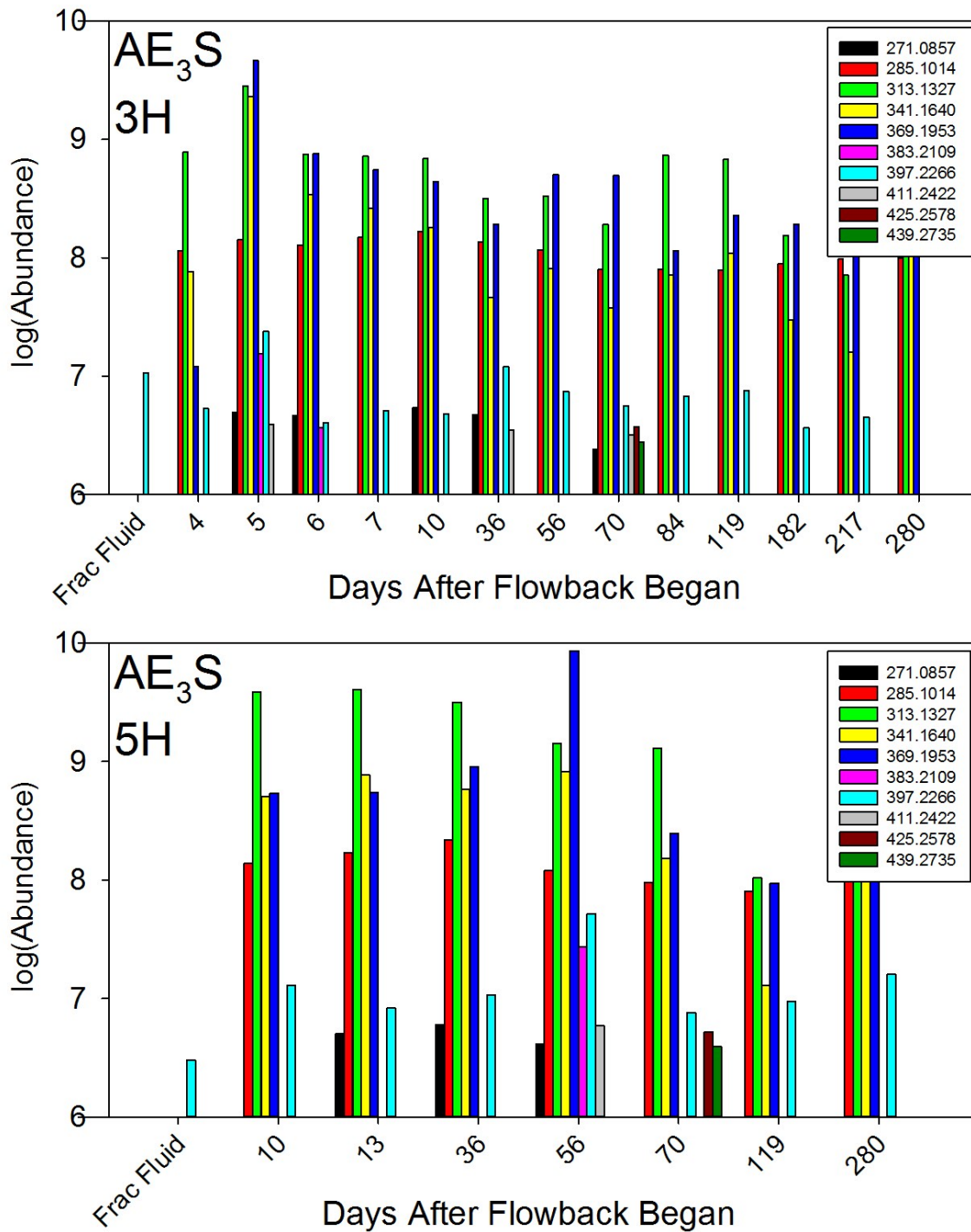


Figure S3. Distribution of ions corresponding to alcohol ethoxysulfate (AE₃S) homologous series in the MSEEL 3H (top) and 5H (bottom) well by days after flowback began .

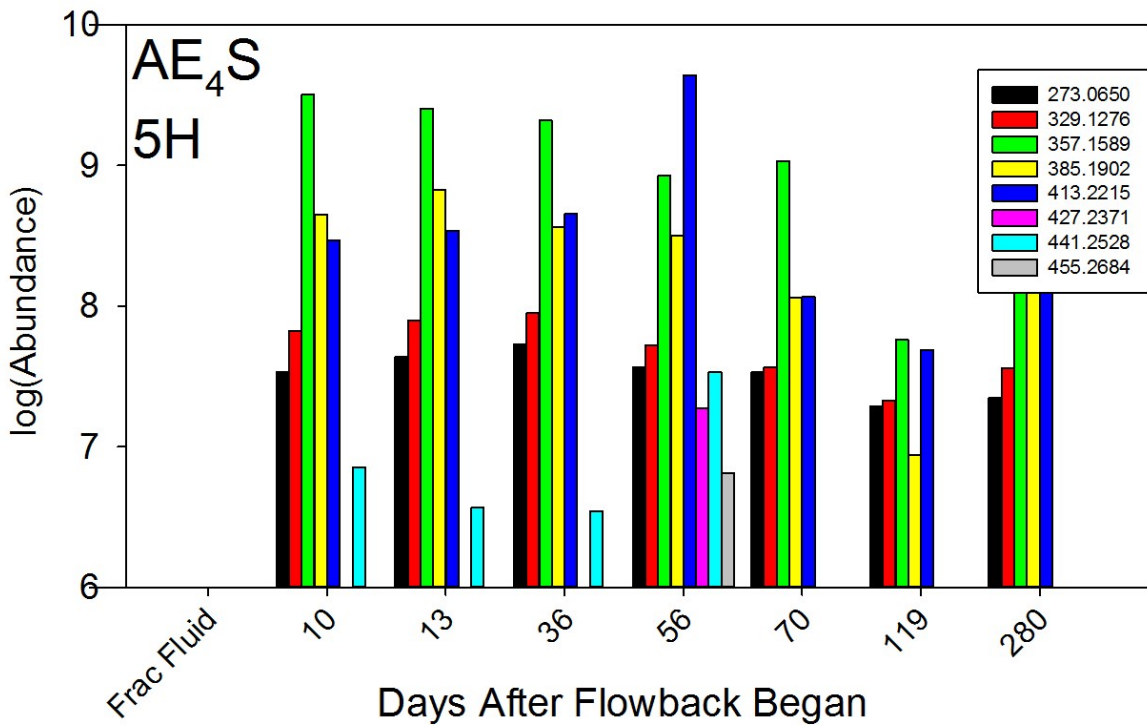
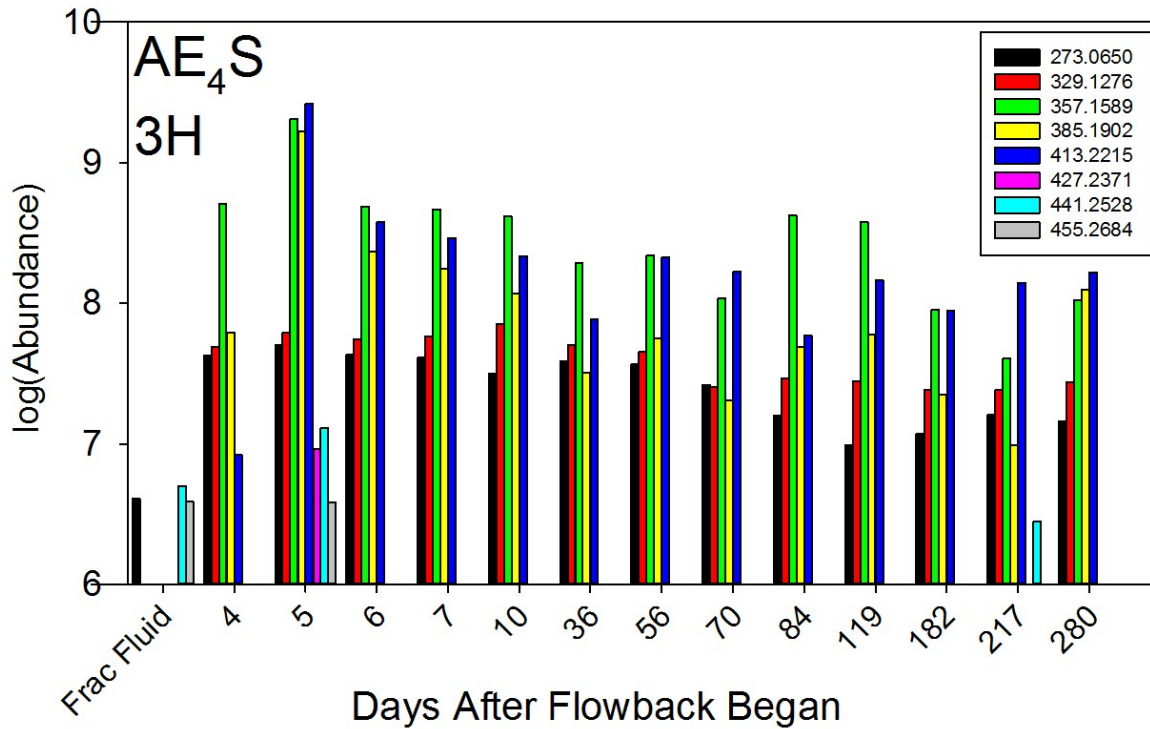


Figure S4. Distribution of ions corresponding to alcohol ethoxysulfate (AE₄S) homologous series in the MSEEL 3H (top) and 5H (bottom) well by days after flowback began.

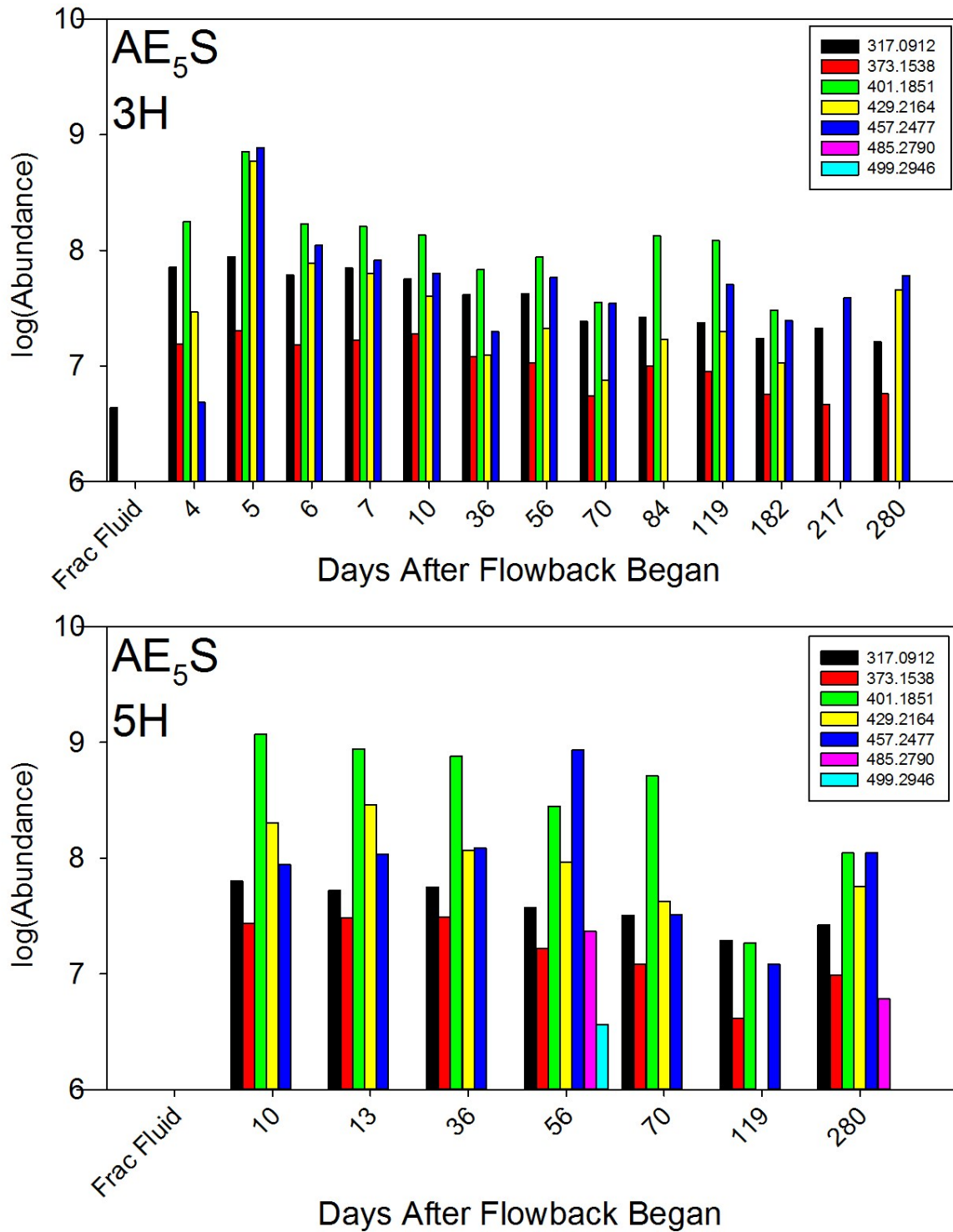


Figure S5. Distribution of ions corresponding to alcohol ethoxysulfate (AE₅S) homologous series in the MSEEL 3H (top) and 5H (bottom) well by days after flowback began.

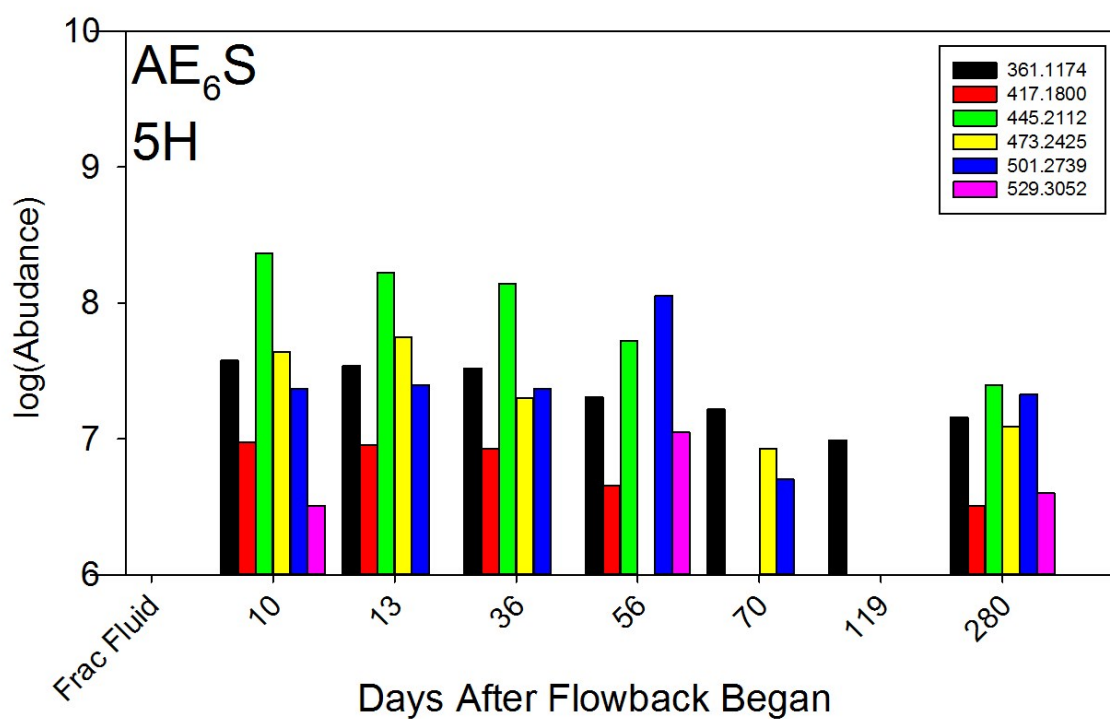
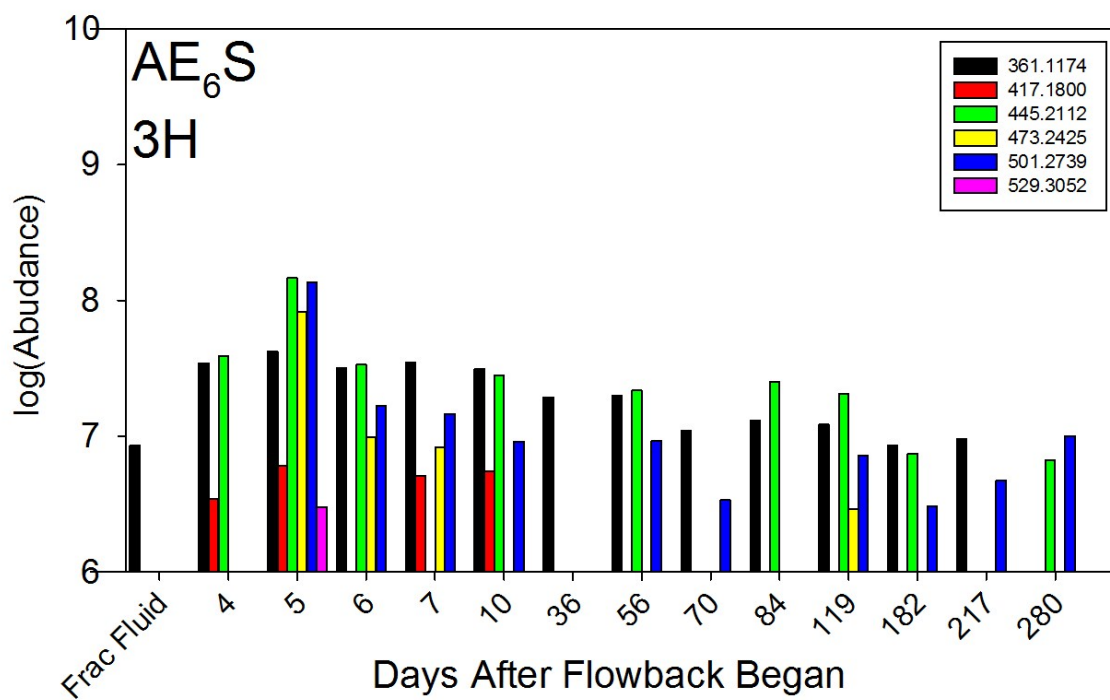


Figure S6. Distribution of ions corresponding to alcohol ethoxysulfate (AE₆S) homologous series in the MSEEL 3H (top) and 5H (bottom) well by days after flowback began.

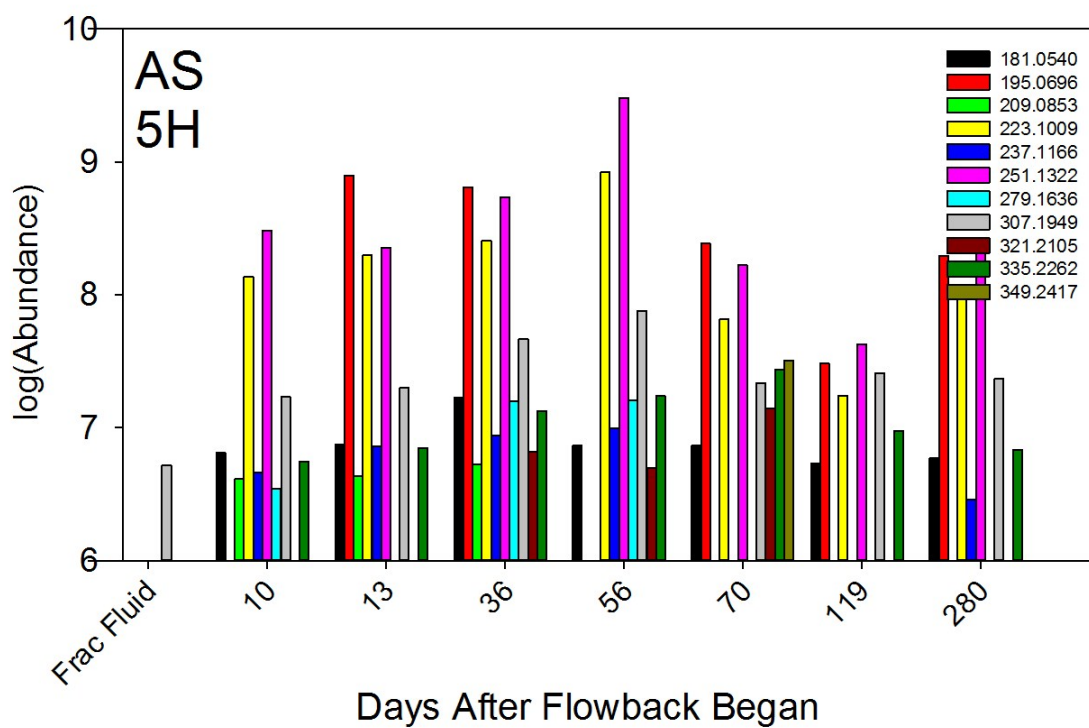
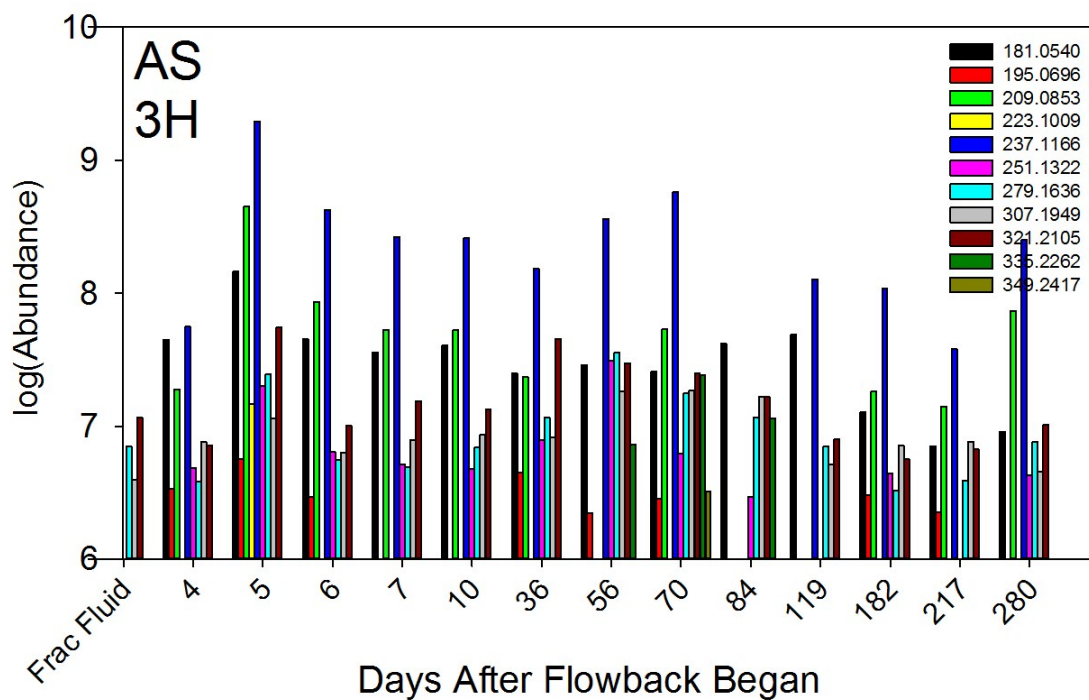


Figure S7. Distribution of ions corresponding to alcohol sulfate (AS) homologous series in the MSEEL 3H (top) and 5H (bottom) well by date.

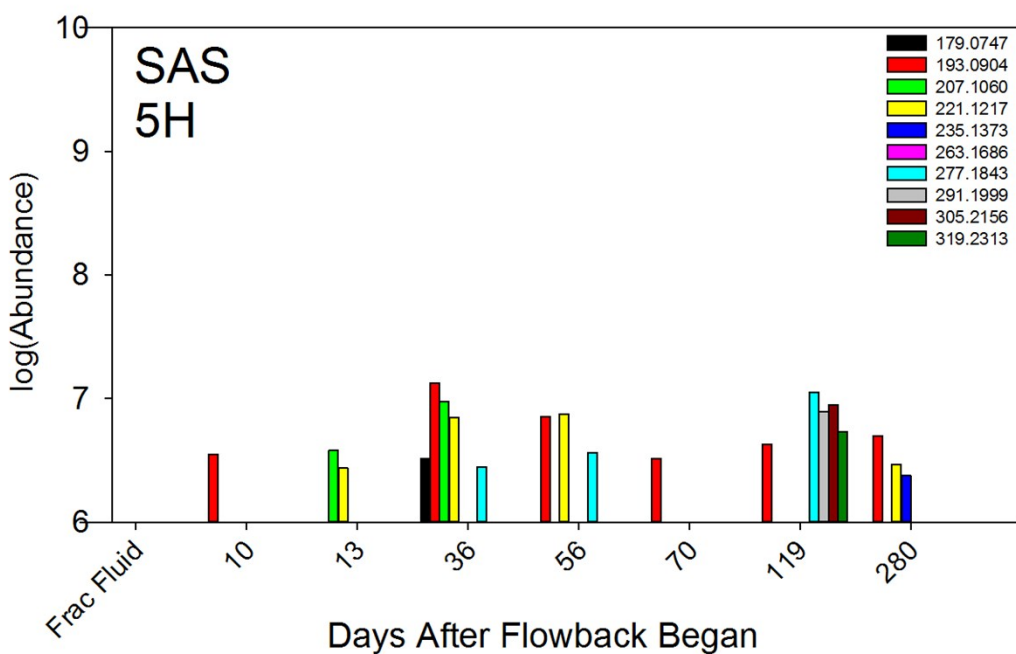
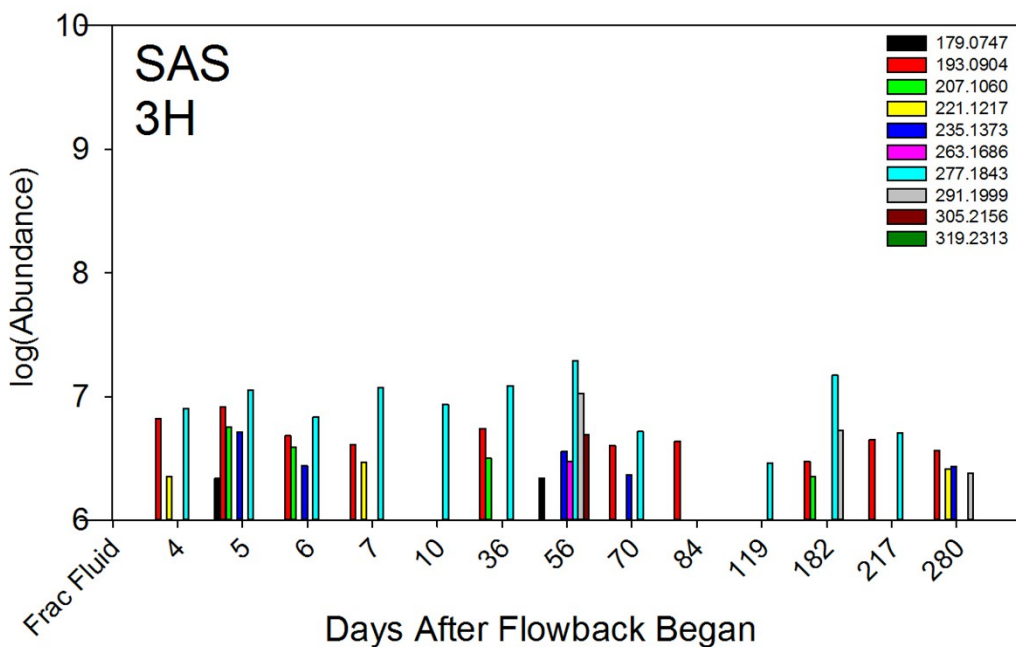


Figure S8. Distribution of ions corresponding to secondary alkane sulfonate (SAS) homologous series in the MSEEL 3H (top) and 5H (bottom) well by date.

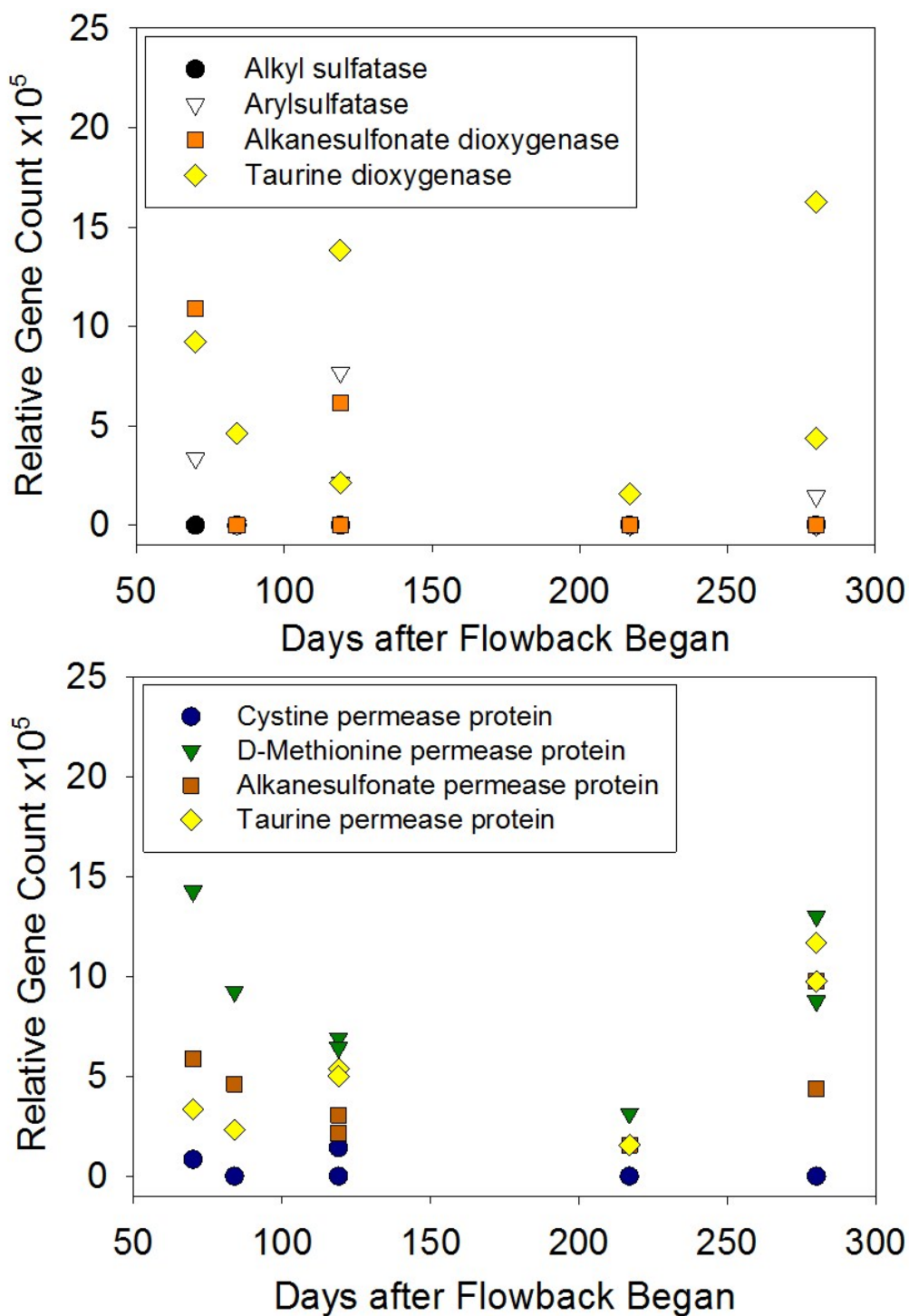


Figure S9. Relative counts for genes associated with organic sulfur cycling identified in Marcellus shale well produced water metagenomes. Genes were identified using KEGG orthology numbers with the exception of alkyl sulfatase (EC number); associated KO and EC numbers and raw counts are given in **Table S5**. Relative gene count values are calculated as the raw gene count divided by the assembled gene count $\times 10^5$.

Supplemental Methods and Results

1. Photochemistry Experiment

Methods. Six MSEEL flowback and produced water solid phase extracts were used for photochemistry experiments. Concentrated and desalted methanolic extracts were evaporated under ultrahigh purity N₂ gas and the dried extract was then reconstituted in MilliQ water followed by sonication for 5 minutes to ensure re-dissolution. Reconstituted samples (3.5 to 11 mg L⁻¹ dissolved organic carbon) were loaded in to a solar simulator irradiation system with semi-continuous flowthrough absorbance and fluorescence excitation emission matrix measurements¹. The solar simulator irradiation system has been described previously in detail¹. It consists of a 1,000 W Xe arc lamp with a 1.5 air mass filter (AM 1.5) to match the direct and diffuse solar spectrum at the Earth surface at a zenith angle of 48.2°, and an intensity of 850 W m⁻². The irradiation cell consists of a custom-built circular borosilicate flow cell, 2mm wide by 1mm deep, with a surface area of 101 cm², and is temperature controlled at 25 °C. This system is directly connected to an Aqualog spectrofluorometer (Horiba Jobin Yvon Instruments) and sample fluid continuously circulates between the irradiation flowcell and the spectrofluorometer. Actinometry measurements (*p*-nitroanisole/pyridine) indicated that the light intensity measured at the irradiation cell is approximately 76% of the measured irradiation (850 W m²), equivalent to the fraction of fluid in the flowcell (receiving light) versus the tubing and spectrophotometer (not receiving light) at any given time ¹. Absorbance and fluorescence measurements were collected every 20 minutes to indicate changes in solution chemistry. Reconstituted extracts from before and after the photoirradiation experiments (15 mL) were extracted using Bond Elut PPL cartridges (200 mg/3 mL) as described in Section 2.1.

Results. The smaller fluid volumes and potentially lower extraction efficiencies resulted in lower

abundances in the overall mass spectra pre-irradiation (15 mL) compared to the original samples (200 mL). However, the highest AES/AS surfactant abundances in the T0 samples corresponded to those highest in the original MSEEL samples (e.g., C12-AE1S, C12-AE2S C12-AE3S), indicating that the evaporation and reconstitution of the methanolic extracts indeed contained these surfactants. Following 20 hr solar irradiation experiments of the six flowback and produced water extracts, changes in the abundances of AES were observed. In the two T0 samples that had the highest AES abundances, a decrease was observed in AES and AS abundances (**Figure S10**). However, there was no consistent trend in the other produced water samples, likely due to their lower initial abundances within the complex mixtures and the sensitivity of the FT-ICR-MS. The rate of photodegradation of AES is not reported in the literature, but a photo-Fenton treatment strategy for AEO removal in wastewaters indicated substantial mineralization². These results are limited to the desalted organic extracts, limiting the application of these results. In a natural setting, the presence of the more complex inorganic matrix and other natural factors (e.g., sorption, turbidity) could influence the fate of AES/AS surfactants and other organic compounds.

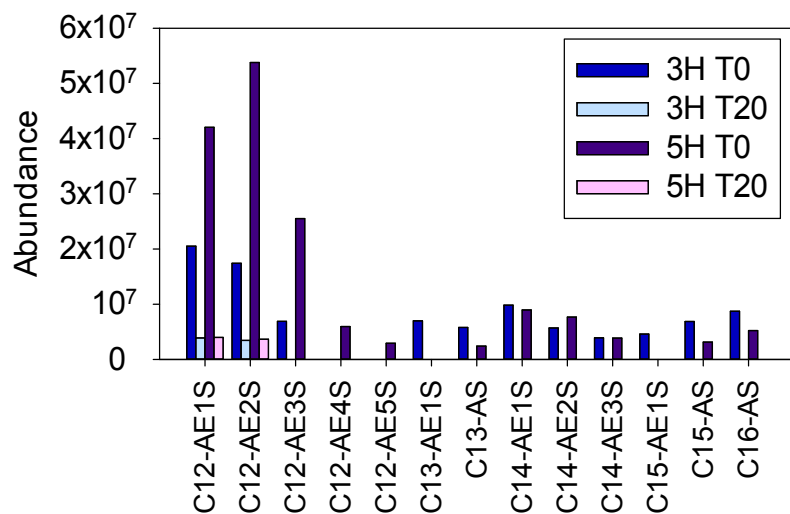


Figure S10. Abundance of AES and AS abundances present in Day 280 produced water (3H well) and Day 13 flowback (5H well) samples before and after 20 hr photoirradiation.

2. Anaerobic Biodegradation Experiment

Methods. Subsamples were collected from anaerobic biodegradation experiments of hydraulic fracturing fluid additives in a pseudo-spill environment³. Briefly, a synthetic hydraulic fracturing fluid was mixed with agricultural soil cores collected from Port Columbus International Airport and stored anaerobically. Fluid subsamples (10 mL) were collected on days 0, 14, and 50 and immediately filtered (0.22µm PES filter, EMD Millipore) and frozen for non-target analyses. Frozen extracts were later thawed and solid phase extracted using Bond Elut PPL cartridges (200 mg/3 mL) in the same manner as described in section 2.1. Quality control procedures for this experiment included confirming the absence of analyte ions from ground water and soil background samples and comparing the biotic changes to those observed under abiotic conditions.

Results. Sample extracts from a fracturing fluid anaerobic biodegradation mesocosm experiment focusing on glycols and alcohol ethoxylates³ were also analyzed using FT-ICR-MS. This allowed for the investigation of additional compounds not targeted using the LC-MS techniques of the original study including AES. The fracturing fluid mixture used in this study³, a mixture common to the Marcellus shale region, contained a commercially available corrosion inhibitor and a stimulation surfactant that both list ethoxylated alcohols on their SDS sheets. AES were also identified in these samples based on exact mass alongside the expected alcohol ethoxylates (AEOs). Fragmentation of the AES ions in these sample extracts revealed a dominant ion at m/z 97, the expected fragment from AES⁴. Tracking of AES abundance over the 50 day time series revealed a substantial decrease in AES ion abundance following the 50 day incubation (**Figure S11**), mirroring the trends measured for C₈AEOs and C₁₀AEOs³. AES can be degraded under

anaerobic conditions,⁵ supporting that the suggestion this decrease in AES ion abundance reflects actual degradation although the FT-ICR-MS analysis was only at best semi-quantitative.

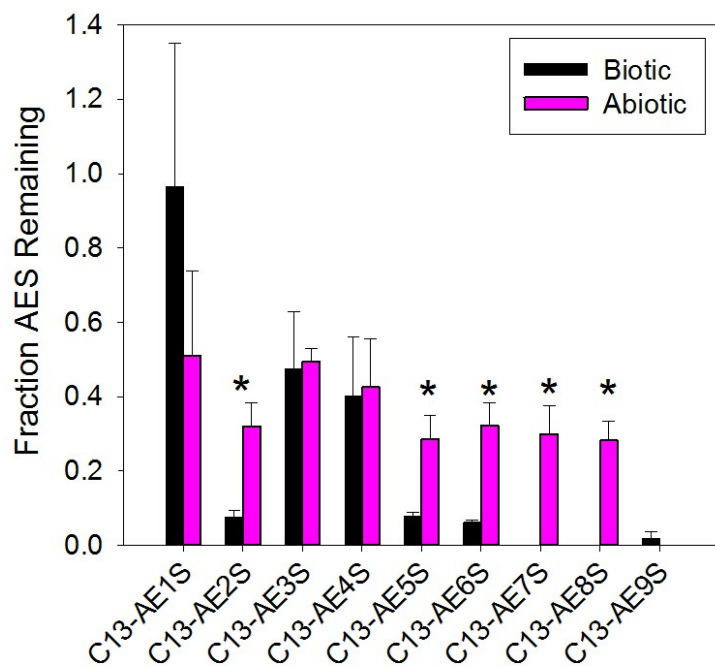


Figure S11. Fraction of C₁₃AES compounds remaining (based on raw abundance/peak intensity) following 50-day anaerobic biodegradation mesocosm experiment (n=3)³. *Indicates biotic is significantly lower than abiotic at $\alpha=0.05$ level (paired t-test, one-sided).

References

- 1 S. A. Timko, M. Gonsior and W. J. Cooper, *Water Res.*, 2015, **85**, 266–274.
- 2 S. S. da Silva, O. Chiavone-Filho, E. L. de Barros Neto, A. L. N. Mota, E. L. Foletto and C. A. O. Nascimento, *Environ. Technol.*, 2014, **35**, 1556–1564.
- 3 K. M. Heyob, J. Blotevogel, M. Brooker, M. V. Evans, J. J. Lenhart, J. Wright, R. Lamendella, T. Borch and P. J. Mouser, *Environ. Sci. Technol.*, 2017, **51**, 13985–13994.
- 4 P. A. Lara-Martín, A. Gómez-Parra and E. González-Mazo, *J. Chromatogr. A*, 2006, **1137**, 188–197.
- 5 *Alcohol Ethoxysulphates (AES) Environmental Risk Assessment*, HERA, 2004.